Inorg. Chem. **2005**, *44*, 4534–4545

Rational Synthesis and Magnetic Properties of a Family of Low-Dimensional Heterometallic Cr–Mn Complexes Based on the Versatile Building Block $[Cr(2,2'\text{-bipyridine})(CN)_4]^-$

Yuan-Zhu Zhang,[†] Song Gao,*[,†] Zhe-Ming Wang,[†] Gang Su,[‡] Hao-Ling Sun,[†] and Feng Pan[†]

State Key Laboratory of Rare Earth Materials Chemistry and Applications and PKU-HKU Joint Laboratory on Rare Earth Materials and Bioinorganic Chemistry, College of Chemistry and Molecular Engineering, Peking University, Beijing 100871, P. R. China, and College of Physical Sciences, Graduate School of the Chinese Academy of Sciences, P.O. Box 3908, Beijing 100039, P. R. China

Received November 11, 2004

Six heterometallic compounds based on the building block $[Cr(bpy)(CN)_4]^-$ (bpy = 2,2′-bipyridine) with secondary and/or tertiary coligands as modulators, $\{Mn(H_2O)_2[Cr(bpy)(CN)_4]_2\}_n$ (**1**), $\{Mn(bpy)(H_2O)[Cr(bpy)(CN)_4]_2 \cdot H_2O\}_n$ (**2**), $[Mn(bpy)_2][Cr(bpy)(CN)_4]_2 \cdot 5H_2O$ (**3**), $\{[Mn(dca)(bpy)(H_2O)][Cr(bpy)(CN)_4] \cdot H_2O\}_n$ (**4**) (dca = $N(CN)_2^-$), $\{Mn(N_3)(CH_3OH)[Cr(bpy)(CN)_4] \cdot 2H_2O\}_n$ (**5**), and $\{Mn(bpy)(N_3)(H_2O)[Cr(bpy)(CN)_4] \cdot H_2O\}_2$ (**6**), have been prepared and characterized structurally and magnetically. X-ray crystallography reveals that the compounds **1**, **2**, **4**, and **5** consist of one-dimensional (1D) chains with different structures: a 4,2-ribbon-like chain, a branched zigzag chain, a 2,2-CC zigzag chain, and a 3,3-ladder-like chain,[1b] respectively. It also reveals that compound **3** has a trinuclear $[MnCr_2]$ struture, and compound **6** has a tetranuclear $[Mn_2Cr_2]$ square structure. Magnetic studies show antiferromagnetic interaction between Cr^{III} and Mn^{II} ions in all compounds. All of the chain compounds exhibit metamagnetic behaviors with different critical temperatures (T_c) and critical fields (H_c; at 1.8 K): 3.2 K and 3.0 kOe for **1**; 2.3 K and 4.0 kOe for **2**; 2.1 K and 1.0 kOe for **4**; and 4.7 K and 5.0 kOe for **5**, respectively. The noncentrosymmetric compound **2** is also a weak ferromagnet at low temperature because of spin canting. The magnetic analyses reveal Cr–Mn intermetallic magnetic exchange constants, J, of –4.7 to –9.4 cm^{-1} ($H = -JS_{Cr} \cdot S_{Mn}$). It is observed that the antiferromagnetic interaction through the Mn–N–C–Cr bridge increases as the Mn–N–C angle (θ) decreases to the range of 155–180°, obeying an empirical relationship: $J = -40 + 0.2\theta$. This result suggests that the best overlap between t_{2g} (high-spin Mn^{II}) and t_{2g} (low-spin Cr^{III}) occurs at an angle of ~155°.

Introduction

There has been great interest in cyanide-bridged bimetallic assemblies because of their rich structures[1−11] and their increasing importance in the field of molecular magnetic materials such as highest T_c molecule-based materials,[2−4] molecule-based photomagnets,[5] spin crossover materials,[6] single-molecule magnets (SMMs),[7] and single-chain magnets (SCMs).[8] However, the magneto-structural correlation of this large family remains somewhat unclear because the discrete polynuclear molecules and suitable cyanide-bridged chain compounds that can provide genuine examples to test models are not easily obtained through a general synthetic approach

* To whom correspondence should be addressed. E-mail: gaosong@pku.edu.cn. Fax: 86−10−62751708.
† Peking University.
‡ Graduate School of the Chinese Academy of Sciences.

(1) (a) Ohba, M.; Ōkawa, H. *Coord. Chem. Rev.* **2000**, *198*, 313, and references therein. (b) Černák, J.; Orendáč, M.; Potočňák, I.; Chomič, J.; Orendáčová, A.; Skoršepa, J.; Feher, A. *Coord. Chem. Rev.* **2002**, *224*, 51, and references therein. (c) Ma, B. Q.; Gao, S.; Su, G.; Xu, G. X. *Angew. Chem., Int. Ed.* **2001**, *40*, 434.

(2) (a) Gadet, V.; Mallah, T.; Castro, I.; Verdaguer, M.; Veillet, P. *J. Am. Chem. Soc.* **1992**, *114*, 9213. (b) Mallah, T.; Thiebaut, S.; Verdaguer, M.; Veillet, P. *Science* **1993**, *262*, 1554. (c) Entley, W. R.; Girolami, G. S. *Science* **1995**, *268*, 397. (d) Ferlay, S.; Mallah, T.; Quahès, R.; Veillet, P.; Verdaguer, M. *Nature* **1995**, *378*, 701. (e) Sato, O.; Iyoda, T.; Fujishima, A.; Hashimoto, K. *Science* **1996**, *271*, 49.

10.1021/ic0484194 CCC: $30.25
Published on Web 05/26/2005

based upon the so-called "brick and mortar method" in which $[A(CN)_6]^{n-}$ serves as the bricks and the simple metal ions or the coordinatively unsaturated complex $[B(L_1)]^{m+}$ serves as the mortar. In this approach, it is difficult to use a third coligand (L_2) to adjust the obtained structure. Černák et al. and Ohba et al. have reviewed one-dimensional (1D) cyano-bridged complexes and have shed some explicit light on their topologies, and some novel structures are emerging.[1a,1b,9] The first 1D magnetic bimetallic assembly was studied by Babel et al.,[10a] and an unusual 1D rope-ladder chain was obtained in 1994.[10b] Ohba et al. reported two $Ni^{II}-M^{III}$ (M = Fe, Cr) chains with 2,2-TC structure[1b] for a magneto-structural correlation.[11] The exchange interaction parameter, *J*, for Cr−C−N−Ni was estimated to be 16.4 cm^{-1} by Mallah et al.[12] A rational approach by Marvaud et al. resulted in a series of clusters and gave a *J* value of −9 cm^{-1} for $Mn^{II}-N-C-Cr^{III}$, which, in fact, is close to that obtained by the general approach ($[A(CN)_6]^{n-} + [B(L_1)]^{m+}$).[13]

An alternative approach that has encouraged recent interest is one in which $[M(CN)_xL_y]^{n-}$ (M = Cr^{III}, $Fe^{II/III}$, Ru^{III}, Mo^{III}; L = chelate ligand; and x = 2, 3, 4) can be used as the "bricks" to synthesize low-dimensional cyanide-bridged bimetallic compounds. To date, a series of bimetallic assemblies in this new family with interesting magnetic properties have been reported: (1) clusters, including high-nuclearity metal−cyanide cages and high-spin trinuclear, tetranuclear, and heptanuclear complexes;[14,15] (2) four types of 1D chains: the crossed triple-chain $\{Mn[Cr(Me_3tacn)(CN)_3]_3\}_n$ (tacn = 1,4,7-triazacyclononane);[14d] the bimetallic crossed double-chain schemed as 2,4-ribbon[1b] $\{[M^{III}(L)(CN)_4]_2M'^{II}(H_2O)_2\}\cdot 4H_2O$ [M = Fe; M′ = Mn, Co, and Zn, with L = 1,10-phenanthroline (phen), 2,2′-bipyridine (bpy); M = Cr, M′ = Mn, with L = phen] in which the cobalt derivatives show SCM-like properties;[8a,16,17] the bis double-zigzag chain compound $\{[Fe^{III}(bpy)(CN)_4]_2M^{II}(H_2O)\}\cdot MeCN\cdot 0.5H_2O$ (M = Zn, Mn, and Co), exhibiting metamagnetism with T_c = 7 K and H_c = 600 Oe;[8b,15c] and the ladder-like chain compound schemed as 3,3-ladder [1b] $[Fe^{III}(bpca)(CN)_3]Mn^{II}(H_2O)_3$ $[Fe^{III}(bpca)(CN)_3]\cdot 3H_2O$ [bpca = bis(2-pyridyl carbonyl)amidate], exhibiting a ferromagnetic ordering below 2.0 K;[18] (3) a novel two-dimensional (2D) compound, which is the first mixed cyano/azido-bridged coordination polymer, $\{Mn(N_3)(CH_3OH)[Cr(phen)(CN)_4]\cdot CH_3OH\}_n$, exhibiting metamagnetism with T_c = 21 K and H_c = 5 kOe at 1.8 K.[17]

Since these exciting results were first reported, some considerations have developed in this remarkable field. (1) Substituting Cr^{III} for Fe^{III} is an effective means of increasing the strength of the magnetic exchange coupling, which was confirmed by the two isostructural compounds $\{[M^{III}(phen)(CN)_4]_2Mn^{II}(H_2O)_2\}\cdot 4H_2O$ (M = Fe, Cr) in which the latter compound shows a long-range ordering below 3.4 K, whereas the former has no such ordering observed down to 2 K.[16,17] (2) The dimensionalities and the structural characteristics are still limited, in contrast with the coordination diversities of the tailored four-cyanometalate in Scheme 1. Until now, only three modes (mono, cis, and fac) have been observed.[15−17] (3) Our previous results demonstrate that it is possible to use a neutral or charged secondary ligand, such

(3) (a) Dunbar, K. R.; Heintz, R. A. *Prog. Inorg. Chem.* **1997**, *45*, 283 and references therein. (b) Buschmann, W. E.; Paulson, S. C.; Wynn, C. M.; Girtu, M. A.; Epstein, A. J.; White, H. S.; Miller, J. S. *Chem. Mater.* **1998**, *10*, 1386. (c) Dujardin, E.; Ferlay, S.; Phan, X.; Desplanches, C.; Cartier dit Moulin, C.; Sainctavit, P.; Baudelet, F.; Dartyge, E.; Veillet, P.; Verdaguer, M. *J. Am. Chem. Soc*. **1998**, *120*, 11347. (d) Holmes S. M.; Girolami, G. S. *J. Am. Chem. Soc.* **1999**, *121*, 5593.

(4) (a) Ohba, M.; Usuki, N.; Fukita, N.; Ōkawa, H. *Angew. Chem., Int. Ed.* **1999**, *38*, 1795. (b) Hatlevik, Ø.; Buschmann, W. E.; Zhang, J.; Manson, J. L.; Miller, J. S. *Adv. Mater*. **1999**, *11*, 914. (c) Kou, H. Z.; Gao, S.; Zhang, J.; Wen, G. H.; Su, G.; Zheng, K. R.; Zhang, X. X. *J. Am. Chem. Soc.* **2001**, *123*, 11809.

(5) (a) Sato, O.; Iyoda, T.; Fujishima, A.; Hashimoto, K. *Science* **1996**, *272*, 704. (b) Sato, O.; Einaga, Y.; Iyoda, T.; Fujishima, A.; Hashimoto, K. *Inorg. Chem.* **1999**, *38*, 4405. (c) Shimamoto, N.; Ohkoshi, S.; Sato, O.; Hashimoto, K. *Inorg. Chem.* **2002**, *41*, 678. (d) Yokoyama, T.; Okamoto, K.; Ohta, T.; Ohkoshi, S.; Hashimoto, K. *Phys. Rev. B* **2002**, *65*, 064438. (e) Sato, O. *Acc. Chem. Res.* **2003**, *36*, 692 and references therein.

(6) (a) Niel, V.; Thompson, A. L.; Muñoz, M. C.; Galet, A.; Goeta, A. E.; Real, J. A. *Angew. Chem., Int. Ed.* **2003**, *42*, 3760. (b) Molnár, G.; Niel, V.; Gaspar, A. B.; Real, J. A.; Zwick, A.; Bousseksou A.; McGarvey, J. J. *J. Phys. Chem. B* **2002**, *106*, 9701. (c) Molnár, G.; Niel, V.; Real, J. A.; Dubrovinsky, L.; Bousseksou A.; McGarvey, J. J. *J. Phys. Chem. B* **2003**, *107*, 3149.

(7) (a) Sokol, J. J.; Hee, A. G.; Long, J. R. *J. Am. Chem. Soc.* **2002**, *124*, 7656. (b) Berlinguette, C. P.; Vaughn, D.; Canada-Vilalta, C.; Galán-Mascarós, J. R.; Dunbar, K. R. *Angew. Chem., Int. Ed.* **2003**, *42*, 1523. (c) Mironov, V. S.; Chibotaru L. F.; Ceulemans A. *J. Am. Chem. Soc.* **2003**, *125*, 9750. (d) Choi, H. J.; Sokol J. J.; Long, J. R. *Inorg. Chem.* **2004**, *43*, 1606. (e) Schelter, E. J.; Prosvirin, A. V.; Dunbar, K. R. *J. Am. Chem. Soc.* **2004**, *126*, 15004.

(8) (a) Lescouëzec, R.; Vaissermann, J.; Ruiz-Pérez, C.; Lloret F.; Carrasco, R.; Julve, M.; Verdaguer, M.; Dromzee, Y.; Gatteschi, D.; Wernsdorfer, W. *Angew. Chem., Int. Ed.* **2003**, *42*, 1483. (b) Toma, L. M.; Lescouëzec, R.; Lloret, F.; Julve, M.; Vaissermann, J.; Verdaguer, M. *Chem. Commun.* **2003**, 1850. (c) Wang, S.; Zuo, J. L.; Gao, S.; Song, Y.; Zhou, H. C.; Zhang, Y. Z.; You, X. Z. *J. Am. Chem. Soc.* **2004**, *126*, 8900.

(9) (a) Kou, H. Z.; Zhou, B. C.; Gao, S.; Liao, D. Z.; Wang, R. J. *Inorg. Chem.* **2003**, *42*, 5604. (b) Colacio, E.; Domínguez-Vera, J. M.; Lloret, F.; Rodríguez, A.; Stoeckli-Evans, H. *Inorg. Chem.* **2003**, *42*, 6962.

(10) (a) Babel, D.; Kurtz, W. *Stud. Inorg. Chem.* **1983**, *3*, 593. (b) Ohba, M.; Maruono, N.; Ōkawa, H.; Enoki, T.; Latour, J. M. *J. Am. Chem. Soc.* **1994**, *114*, 11566.

(11) Ohba, M.; Usuki, N.; Fukita, N.; Ōkawa, H. *Inorg. Chem.* **1998**, *37*, 3349.

(12) Mallah, T.; Auberger, C.; Verdaguer, M.; Veillet, P. *J. Chem. Soc., Chem. Commun.* **1995**, 61.

(13) (a) Marvaud, V.; Decroix, C.; Scuiller, A.; Guyard-Duhayon, C.; Vaissermann, J.; Gonnet, F.; Verdaguer, M. *Chem.—Eur. J.* **2003**, *9*, 1677. (b) Marvaud, V.; Decroix, C.; Scuiller, A.; Tuyèras, F.; Guyard-Duhayon, C.; Vaissermann, J.; Marrot, J.; Gonnet, F.; Verdaguer, M. *Chem.—Eur. J.* **2003**, *9*, 1692.

(14) (a) Heinrich, J. L.; Berseth, P. A.; Long, J. R. *Chem. Commun.* **1998**, 1231. (b) Berseth, P. A.; Sokol, J. J.; Shores, M. P.; Heinrich, J. L.; Long, J. R. *J. Am. Chem. Soc.* **2000**, *122*, 9655. (c) Sokol, J. J.; Shores, M. P.; Long, J. R. *Angew. Chem., Int. Ed.* **2001**, *40*, 236. (d) Sokol, J. J.; Shores, M. P.; Long, J. R. *Inorg. Chem.* **2002**, *41*, 3052. (e) Heinrich, J. L.; Sokol, J. J.; Hee, A. G.; Long, J. R. *J. Solid State Chem.* **2001**, *159*, 293.

(15) (a) Oshio, H.; Tamada, O.; Onodera, H.; Ito, T.; Ikoma, T.; Tero-Kubota, S. *Inorg. Chem.* **1999**, *38*, 5686. (b) Oshio, H.; Yamamoto, M.; Ito, T. *Inorg. Chem.* **2002**, *41*, 5817. (c) Lescouëzec, R.; Lloret, F.; Julve, M.; Vaissermann, J.; Verdaguer, M. *Inorg. Chem.* **2002**, *41*, 818. (d) Lescouëzec, R.; Vaissermann, J.; Lloret, F.; Julve, M.; Verdaguer, M. *Inorg. Chem.* **2002**, *41*, 5943. (e) Karadas, F.; Schelter, E. J.; Prosvirin, A. V.; Bacsa, J.; Dunbar, K. R. *Chem. Commun.* **2005**, 1414.

(16) (a) Lescouëzec, R.; Lloret, F.; Julve, M.; Vaissermann, J.; Verdaguer, M.; Llusar, R.; Uriel, S. *Inorg. Chem.* **2001**, *40*, 2065. (b) Toma, L.; Lescouëzec, R.; Vaissermann, J.; Delgado, F. S.; Ruiz-Pérez, C.; Carrasco, R.; Cano, J.; Lloret, F.; Julve, M. *Chem.—Eur. J.* **2004**, *10*, 6130.

(17) Zhang, Y. Z.; Gao, S.; Sun, H. L.; Su, G.; Wang Z. M.; Zhang, S. W. *Chem. Commun.* **2004**, 1906.

(18) Lescouëzec, R.; Vaissermann, J.; Toma, L. M.; Carrasco, R.; Lloret, F.; Julve, M. *Inorg. Chem.* **2004**, *43*, 2234.

Scheme 1

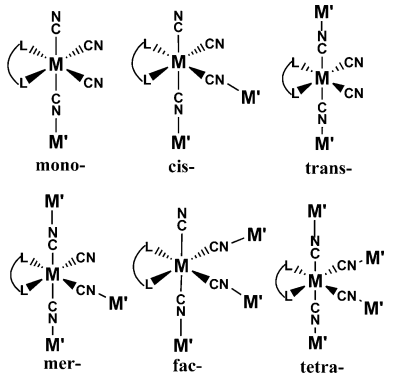

Scheme 2

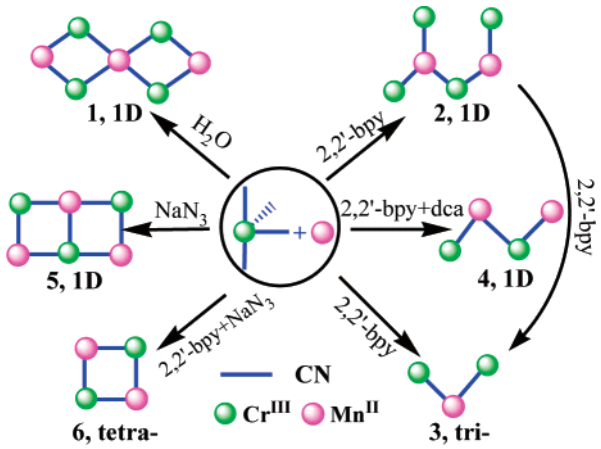

as 2,2′-bpy, 4,4-bpy, N_3^-, $N(CN)_2^-$, or $C_2O_4^{2-}$, together with cyanide groups to adjust the structures.[17] (4) A natural consideration is whether a third coligand can be used to adjust the structures further to obtain genuine samples to test models and provide feedback regarding their magneto-structural correlations as well as develop new models. Here, our approach to synthesis has been illustrated in Scheme 2, in which the black solid arrows depict our synthetic routes. In this article, we report the synthesis, structural characteristics, and magnetic properties of four Mn−Cr chains and two Mn−Cr clusters based on the building block $[Cr(bpy)(CN)_4]^-$.

Results and Discussion

Crystal Structures. Detailed crystallographic data for all compounds are listed in Table 1. Selected bond lengths and angles are listed in Table 2.

Description of the Structure of 1. The structure of compound **1** is made up of neutral cyano-bridged crossed $Mn^{II}-Cr^{III}$ double zigzag chains. It is similar to $[Fe^{III}L(CN)_4]_2[M^{II}(H_2O)_2]\cdot 4H_2O$ (L = phen, 2,2′-bpy; M = Mn, Co, Zn) and $[Cr^{III}(phen)(CN)_4]_2[Mn^{II}(H_2O)_2]\cdot 4H_2O$.[8,16,17] This type of structure has been described as a 4,2-ribbon-like chain. [1b] As shown in Figure 1, each $[Cr(bpy)(CN)_4]^-$ unit connects to two Mn^{II} ions in a cis-geometry in which two of the CN^- ligands remain intact. Each octahedral six-coordinated Mn^{II} is linked to four $[Cr(bpy)(CN)_4]^-$ units at its equatorial positions, and its two axial positions are occupied by two H_2O molecules. Compared with the $[Cr_2Mn]$−phen compound,[17] the Mn−N−C−Cr angles of Mn−N−C (139.57−140.93°) and N−C−Cr (169.18−172.39°) are more bent, and there are no crystallized water molecules, which results in shorter intrachain Cr···Mn, Cr···Cr, and Mn···Mn separations (5.05, 6.26, and 7.94 Å, respectively) and a shorter interchain M···M (Cr···Mn) distance (7 Å). Each chain interacts with four other adjacent chains via hydrogen bonds between O_{water} and N_{cyano}(intact), with O···N = 2.778 Å. Therefore, the 3D structure can be described as H-bonded linkages of 1D double zigzag chains (Supporting Information Figure S1).

Description of the Structure of 2. The structure of compound **2** consists of neutral branched zigzag chains $\{[Mn(bpy)(H_2O)][Cr(bpy)(CN)_4]_2\}_n$ and water molecules of crystallization. As shown in Figure 2, one of the $[Cr(bpy)(CN)_4]^-$ units (Cr2) and Mn^{II} are connected to each other through cyanide groups in cis-geometry corresponding to both Cr and Mn, thus forming a zigzag chain. Another $[Cr(bpy)(CN)_4]^-$ unit (Cr1) is monodentated to Mn as a branch of the chain. Three $N_{cyanide}$ atoms (N_1, N_4, N_5), two N_{bpy} atoms (N_{13} and N_{14}), and one O_{water} atom (O_1) complete the octahedral coordination of Mn^{II}. The angle ∠Mn−N5−C5 (154.9°) from the monodentate $[Cr(bpy)(CN)_4]^-$ (Cr1) is much smaller than those of ∠Mn−N1−C1 (173.5°) and ∠Mn−N4−C4 (170.0°) from the cis unit (Cr2). The Mn−O_{water} and Mn−N_{cynide} bond lengths (2.24 and 2.175−2.257 Å, respectively) are similar to those observed in the former complexes. The adjacent intrachain Cr···Mn, Cr···Cr, and Mn···Mn separations are 5.21−5.46, 8, and 8 Å, respectively. The shortest interchain M···M distance is larger than 7.3 Å. Each chain interacts with two other adjacent chains by $\pi-\pi$ stacking from bpy···bpy with interlayer distances in the range of 3.30−3.58 Å, thus forming a 2D layer.[19] Hydrogen bonds are only found in the layer between the coordinated, crystallized water molecules and the one intact cyanide group. The layers are packed into a three-dimensional (3D) crystal structure along the *c* axis with van der Waals contact (Supporting Information Figure S2).

Description of the Structure of 3. The structure of compound **3** is made up of neutral molecular trinuclear entities of $[Mn(bpy)_2][Cr(bpy)(CN)_4]_2$ and water molecules of crystallization. As shown in Figure 3, both of the $[Cr(bpy)(CN)_4]^-$ units (Cr1 and Cr2) connect to one Mn^{II} ion in a mono-geometry mode. The manganese atom is hexacoordinated with two cyanide nitrogen atoms in cis-positions and four nitrogen atoms from two bpy ligands occupying the other sites, forming a slightly distorted octahedral surrounding. Selected bond lengths and angles are listed in Table 2, and are similar to those observed in the above compounds. The values of the angles between Mn−N_4−C_4 (170.7°) and Mn−N_{11}−C_{35} (164.9°) are slightly deviated from linearity. The intramolecular Cr···Mn and Cr···Cr separations are 5.4 and 8.6 Å, respectively. The trinuclear units are well-isolated, with the shortest intermo-

(19) Roesky, H. W.; Andruh, M. *Coord. Chem. Rev.* **2003**, *236*, 91 and references therein.

Table 1. Summary of Crystallographic Data for the Compounds

	1	2	3	4	5	6
formula	$MnCr_2C_{28}H_{20}N_{12}O_2$	$MnCr_2C_{38}H_{28}N_{14}O_2$	$MnCr_2C_{48}H_{44}N_{16}O_2$	$MnCrC_{26}H_{20}N_{11}O_2$	$MnCrC_{15}H_{18}N_9O_4$	$MnCrC_{24}H_{22}N_{11}O_3$
M_r [g mol^{-1}]	715.50	871.68	1083.93	625.47	495.32	619.47
crystal system	monoclinic	orthorhombic	monoclinic	monoclinic	triclinic	triclinic
space group	$P2_1/n$	$Pca2_1$	$P2_1/c$	$P2_1/n$	$P\bar{1}$	$P\bar{1}$
centro sym	yes	no	yes	yes	yes	yes
a [Å]	7.9402(1)	17.120(3)	22.3706(9)	16.8628(4)	8.3864(3)	9.5844(2)
b [Å]	15.2698(3)	7.9897(2)	14.3757(4)	7.9593(2)	10.8986(3)	11.959(2)
c [Å]	12.7252(3)	29.789(6)	17.0226(6)	22.5123(8)	12.9321(4)	13.774(3)
α [°]	90	90	90	90	102.0137(11)	65.18(3)
β [°]	94.4183(7)	90	104.8021(11)	109.4386(9)	92.9851(12)	79.35(3)
γ [°]	90	90	90	90	111.6520(11)	73.92(3)
V [Å^3]	1538.29(5)	4074.7(14)	5292.7(3)	2849.28(14)	1063.68(6)	1372.7(5)
Z	2	4	4	4	2	2
ρ_{calcd} [mg m^{-3}]	1.545	1.421	1.360	1.458	1.547	1.499
crystal size [mm^{-1}]	0.5 × 0.3 × 0.25	0.6 × 0.52 × 0.08	0.16 × 0.12 × 0.1	0.2 × 0.18 × 0.05	0.15 × 0.08 × 0.05	0.18 × 0.16 × 0.12
μ(Mo Kα) [mm^{-1}]	1.146	0.881	0.698	0.869	1.145	0.904
θ_{limit} [°]	3.41−27.49	3.48−27.48	3.40−25.02	3.52−27.49	3.40−27.50	1.63−26.29
measured refln	33265	57915	70111	42532	23143	7873
unique refln	3524	9316	8892	6513	4870	5493
observed refln[a]	2659	6052	3263	2639	2589	2849
no. of params	213	516	649	383	279	367
F(000)	722	1772	2228	1272	504	632
GOF	1.015	0.935	0.900	0.914	0.883	1.008
T_{max}/T_{min}	0.756/0.707	0.947/0.783	0.942/0.836	0.959/0.816	0.946/0.906	0.899/0.854
R1[b]	0.0289	0.0402	0.0621	0.0463	0.0370	0.0643
wR2[c]	0.0465	0.0825	0.2319	0.1489	0.0958	0.1182

[a] Observation criterion: $I \geq 2\sigma(I)$. [b] $R1 = \sum||F_o| - |F_c||/\sum|F_o|$. [c] $wR2 = \{\sum[w(F_o^2 - F_c^2)^2]/\sum[w(F_o^2)^2]\}^{1/2}$.

lecular M···M distance being larger than 8.2 Å, and are linked to the 3D crystal struture through rich H-bondings.

Description of the Structure of 4. The structure of compound **4** consists of neutral zigzag chains of $\{[Mn(dca)(bpy)(H_2O)][Cr(bpy)(CN)_4]\}_n$ [dca = $N(CN)_2^-$] and crystallized water molecules, in which the chains are linked through $\pi-\pi$ stacking and H-bonding. This type of structure has been described as 2,2-CC chain.[1b] As shown in Figure 4, the $[Cr(bpy)(CN)_4]^-$ and $[Mn(bpy)(H_2O)(dca)]^+$ units are linked by cyanide groups in cis-geometry along the b axis. The coordination geometry of Mn^{II} is octahedral with two $N_{cynaide}$ atoms (N_1 and N_2), two N_{bpy} atoms (N_7 and N_8), one O_{water} atom (O_1), and one N_{dca} atom (N_9) from the terminal dca. The bond lengths of Cr−C are in the range of 2.063−2.086 Å, and the angels of ∠Cr−C−N (173.7−175.9°) and ∠Mn−N−C (172.7−173.0°) are close to 180°. The average intrachain Cr···Mn, Cr···Cr, and Mn···Mn separations are 5.3, 8, and 8 Å, respectively, and are similar to those of compound **2**. The shortest interchain M···M distance is larger than 7.2 Å. As shown in Supporting Information Figure S3, the chains are aligned along the b axis, and the shortest interchain bpy···bpy distances of 3.4−3.6 Å suggest $\pi-\pi$ stacking, giving a slipped packing along the a axis which is stacked along the c axis by H-bonding from O_1 and the neighboring N_{dca} (N_{11}) ($O_1\cdots N_{11}$ = 2.84 Å) and from $O_1\cdots O_2\cdots N_4$ ($O_1\cdots O_2$ = 2.754 Å; $O_2\cdots N_4$ = 2.915−3.029 Å).[19]

Description of the Structure of 5. The structure of compound **5** consists of neutral $\{Mn(H_2O)(CH_3OH)(N_3)[Cr(bpy)(CN)_4]\}_n$ bimetallic ladder-like chains and crystallized water molecules, in which the chains are connected with H-bonding and van der Waals contact. This type of structure has been described as a 3,3-ladder chain.[1b] As shown in Figure 5, Cr^{III} and Mn^{II} ions are connected through cyanide bridges to a planar ladder-like chain with regularly alternating Mn^{II} and Cr^{III} atoms along the edges. Thus, each $[Cr(bpy)(CN)_4]^-$ unit connects to three Mn^{II} ions in a mer-geometry in which three equatorial cyanide groups are used to connect to three metal ions, and the last one is intact. The polyhedron of six-coordinated Mn^{II} is almost a regular octahedron comprised of three $N_{cyanide}$ atoms (N_2, N_3, N_4), one N_{azide} atom (N_7), one $O_{methanol}$ atom (O_1), and one O_{water} atom (O_2). The $Mn-N_{azide}$ and $Mn-N_{cynide}$ bond lengths are 2.15 and 2.21−2.24 Å, respectively. The bond lengths and angles around the Cr atoms are similar to those of the former complexes, which are listed in Table 1. The rung and leg Cr···Mn distances are slightly different, measuring 5.4 and 5.43−5.47 Å, respectively. The shortest interchain Cr···Cr, Cr···Mn, and Mn···Mn distances are 7.95, 7.90, and 7.82 Å, respectively. As shown in Supporting Information Figure S4, each ladder interacts with two adjacent ladders through H-bonding between N_9 (azide) and O_1 (methanol) with N···O = 2.803 Å in the ac plane, thus forming a 2D double

Table 2. Selected Bond Lengths [Å] and Angles [°]

		1	
$Cr(1)-C_{intact}$	2.051(2)−2.065(2)	$O(1)-Mn(1)-O(1)^a$	180.0
$Cr(1)-N_{bpy}$	2.072−2.076	$C(1)-N(1)-Mn(1)$	140.93(15)
$Cr(1)-C_{bridge}$	2.074−2.087(2)	$C(3)-N(3)-Mn(1)^c$	139.57(15)
$Mn(1)-O(1)$	2.1843(14)	$N(1)-C(1)-Cr(1)$	169.18(16)
$Mn(1)-O(1)^a$	2.1843(14)	$N(2)-C(2)-Cr(1)$	172.39(19)
$Mn(1)-N(3)^b$	2.2412(16)	$N(3)-C(3)-Cr(1)$	172.82(16)
$Mn(1)-N(1)$	2.2573(15)	$N(4)-C(4)-Cr(1)$	174.84(17)
$Mn(1)-N(1)^a$	2.2573(15)		
		2	
$Mn(1)-N(4)^d$	2.175(3)	$N(1)-C(1)-Cr(2)$	174.8(3)
$Mn(1)-N(1)$	2.257(3)	$N(2)-C(2)-Cr(2)$	175.0(4)
$Mn(1)-N(5)$	2.194(3)	$N(3)-C(3)-Cr(2)$	175.7(4)
$Mn(1)-O(1)$	2.239(3)	$N(4)-C(4)-Cr(2)$	176.5(3)
$Mn(1)-N_{bpy}$	2.255(3)−2.261(3)	$N(5)-C(5)-Cr(1)$	169.2(3)
$Cr(1)-N_{bpy}$	2.053(3)−2.078(3)	$N(6)-C(6)-Cr(1)$	174.3(4)
$Cr(1)-C(5)_{bridge}$	2.061(4)	$N(7)-C(7)-Cr(1)$	172.8(4)
$Cr(1)-C_{intact}$	2.062(5)−2.102(5)	$N(8)-C(8)-Cr(1)$	176.2(4)
$Cr(2)-C_{intact}$	2.057(4)−2.059(4)	$C(1)-N(1)-Mn(1)$	173.5(3)
$Cr(2)-N_{bpy}$	2.067(3)−2.071(3)	$C(4)-N(4)-Mn(1)^e$	170.0(3)
$Cr(2)-C(4)_{bridge}$	2.074(4)	$C(5)-N(5)-Mn(1)$	154.9(3)
$Cr(2)-C(1)_{bridge}$	2.083(4)		
		3	
$Mn(1)-N(4)_{bridge}$	2.199(6)	$C(4)-N(4)-Mn(1)$	170.7(6)
$Mn(1)-N(11)_{bridge}$	2.202(6)	$C(35)-N(11)-Mn(1)$	164.9(6)
$Mn(1)-N_{bpy}$	2.223(6)−2.262(5)	$N(4)-C(4)-Cr(1)_{bridge}$	176.3(6)
$Cr(1)-C_{intact}$	2.015(8)−2.065(9)	$N(11)-C(35)-Cr(2)_{bridge}$	176.7(7)
$Cr(1)-N_{bpy}$	2.063(5)−2.075(5)	$N-C-Cr(2)_{intact}$	177.6(10)−179.5(8)
$Cr(2)-C_{intact}$	2.019(10)−2.052(8)	$N-C-Cr(1)_{intact}$	176.0(8)−177.2(8)
$Cr(2)-N_{bpy}$	2.055(6)−2.062(6)		
$Cr(1)-C(4)_{bridge}$	2.087(8)		
$Cr(2)-C(35)_{bridge}$	2.079(8)		
		4	
$Cr(1)-N_{bpy}$	2.073(3)−2.079(3)	$C(1)-N(1)-Mn(1)^d$	173.0(3)
$Cr(1)-C_{bridge}$	2.063(4)−2.086(4)	$C(2)-N(2)-Mn(1)$	172.7(3)
$Cr(1)-C_{intact}$	2.066(4)	$N(1)-C(1)-Cr(1)$	175.9(3)
$Mn(1)-N(9)_{dca}$	2.171(4)	$N(2)-C(2)-Cr(1)$	173.7(3)
$Mn(1)-O(1)$	2.219(3)	$N(3)-C(3)-Cr(1)$	174.6(4)
$Mn(1)-N_{cyanide}$	2.226(3)−2.246(3)	$N(4)-C(4)-Cr(1)$	179.0(4)
$Mn(1)-N_{bpy}$	2.233(3)−2.255(3)		
		5	
$Mn(1)-N(7)_{azide}$	2.151(3)	$N(8)-N(7)-Mn(1)$	150.3(3)
$Mn(1)-O(1)$	2.217(3)	$N(7)-N(8)-N(9)$	175.7(4)
$Mn(1)-O(2)$	2.238(3)	$N(1)-C(1)-Cr(1)$	177.9(3)
$Mn(1)-N(4)$	2.210(3)	$N(2)-C(2)-Cr(1)$	174.0(3)
$Mn(1)-N(2)^f$	2.238(3)	$N(3)-C(3)-Cr(1)$	177.4(3)
$Mn(1)-N(3)^d$	2.244(3)	$N(4)-C(4)-Cr(1)$	176.5(3)
$Cr(1)-C(1)_{intact}$	2.062(4)	$C(2)-N(2)-Mn(1)^f$	166.6(3)
$Cr(1)-N_{bpy}$	2.068(2)−2.070(2)	$C(3)-N(3)-Mn(1)^e$	177.2(3)
$Cr(1)-C_{bridge}$	2.070(3)−2.091(3)	$C(4)-N(4)-Mn(1)$	177.6(3)
		6	
$Mn(1)-N(9)_{azide}$	2.136(6)	$C(2)-N(2)-Mn(1)^g$	161.9(5)
$Mn(1)-O(1)$	2.220(4)	$C(3)-N(3)-Mn(1)$	161.3(6)
$Mn(1)-N(3)$	2.166(5)	$N(1)-C(1)-Cr(1)$	178.3(7)
$Mn(1)-N(2)^a$	2.229(6)	$N(2)-C(2)-Cr(1)$	178.5(6)
$Mn(1)-N_{bpy}$	2.236(5)−2.266(5)	$N(3)-C(3)-Cr(1)$	174.7(6)
$Cr(1)-N_{bpy}$	2.042(5)−2.055(5)	$N(4)-C(4)-Cr(1)$	177.9(6)
$Cr(1)-C_{intact}$	2.051(7)−2.076(7)	$N(11)-N(10)-N(9)$	179.3(8)
$Cr(1)-C_{bridge}$	2.042(7)−2.074(7)		

[a] $-x+1, -y+1, -z+1$. [b] $-x, -y+1, -z+1$. [c] $x-1, y, z$. [d] $x, y+1, z$. [e] $x, y-1, z$. [f] $-x+1, -y+1, -z$. [g] $-x, -y+2, -z+1$.

layer, which is packed into a 3D structure along the *c* axis through van der Waals contact. Here, the azide only serves as a terminal ligand, which is different from that of the 2D complex.[17] This must be because the scarcity of one phenyl cycle abolishes the $\pi-\pi$ stacking.

Description of the Structure of 6. The structure of compound **6** consists of a neutral molecular square with alternating Cr and Mn units bridged by cyanide and crystallized water molecules. As shown in Figure 6, each $[Cr(bpy)(CN)_4]^-$ bridges two Mn^{II} ions in cis-geometry, and each Mn^{II} ion in turn links two $[Cr(bpy)(CN)_4]^-$ in a cis-fashion as well, yielding a slightly distorted square, which can be viewed as a "snippet" of **5.** The coordination surroundings of Cr are similar to those found in the former complexes. The bridging cyano ligands coordinate to the Mn^{II} ion [Mn−N = 2.166(5) and 2.229(6) Å] in a bent fashion, with Mn−N−C bond angles of 161.9(5)° and 161.3(6)°, respectively. The remaining four coordination positions are occupied by two nitrogen

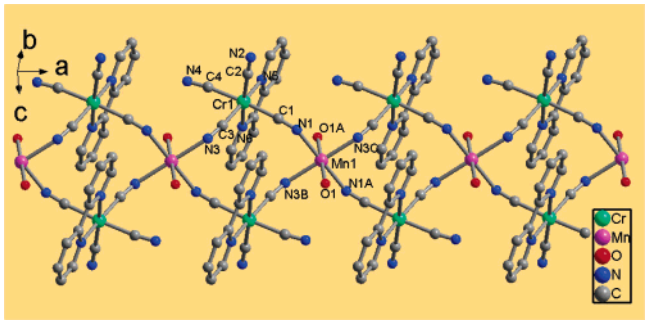

Figure 1. Ball-and-stick structure of the crossed zigzag chains of **1** along the *a* axis.

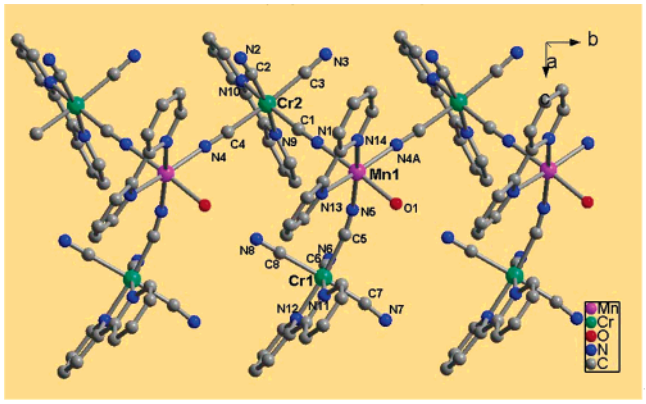

Figure 2. Ball-and-stick structure of the branched zigzag chains of **2** along the *b* axis (crystallized water molecules are omitted).

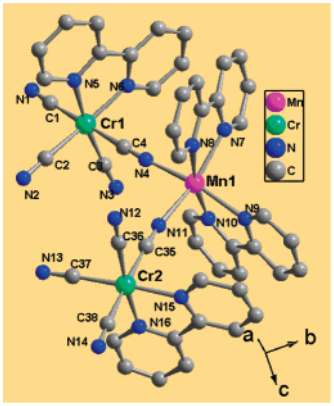

Figure 3. Ball-and-stick trinuclear structure of **3**. (crystallized water molecules are omitted).

atoms from 2,2′-bpy, one nitrogen atom from azide, and one coordinated water oxygen atom with a Mn−O distance of 2.220 Å. The size of the molecular square is ∼5.24 × 5.37 Å. The isolated square is connected through rich H-bonding into a 3D structure, with the shortest intermolecular M···M distance being 7.8 Å.

In our previous communication,[17] we dealt with the magneto-structural correlation for a 4,2-ribbon chain by using the Fisher model; however, more examples were needed for comparison. So, compound **1** was obtained as expected when we used [Cr(bpy)(CN)$_4$]$^-$ instead of [Cr(phen)(CN)$_4$]$^-$ as the building block. By checking this compound carefully, we found that the two water molecules that are coordinated to

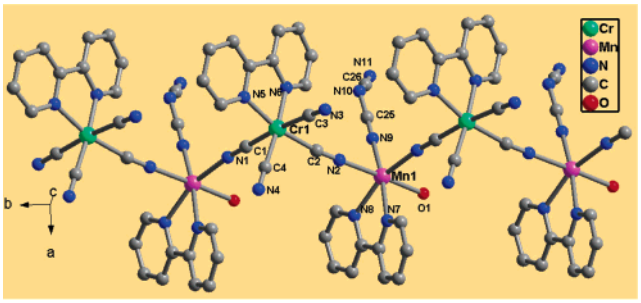

Figure 4. Ball-and-stick structure of the pure zigzag chains of **4** along the *b* axis (crystallized water molecules are omitted).

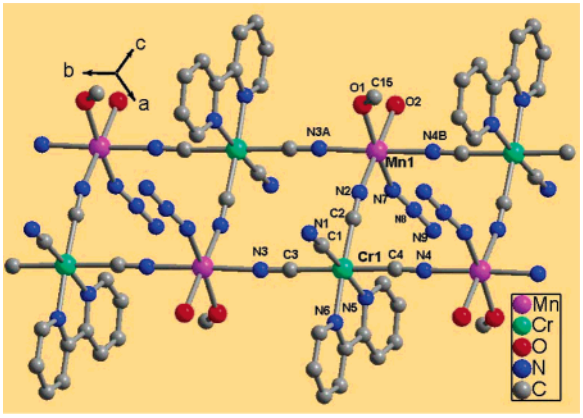

Figure 5. View of the ball-and-stick 3,3-ladder-like chain of **5** (crystallized water molecules are omitted).

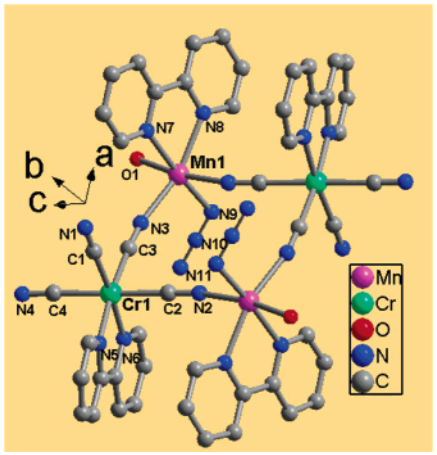

Figure 6. Ball-and-stick square-like crystal structure of **6** (crystallized water molecules are omitted).

each Mn^{II} ion could be substituted easily, which led us to carry out a rational synthesis of this family of compounds with low dimensions. At first, we used a chelate ligand of 2,2′-bpy to replace the coordination water molecules, and as a result, the branched zigzag chain of compound **2** was isolated (when the ratio of 2,2′-bpy and Mn^{II} was 1). Obviously, **2** can be seen as a derivative of **1** in which one of the crossed chains was snipped by bpy. When the ratio exceeded 2, the trinuclear compound **3** was isolated. We then addressed the question, Can the branch of [Cr(bpy)(CN)$_4$]$^-$ in **2** be substituted by an anion? When Na(dca) was added, we succeeded in our rational synthesis of a pure zigzag chain

Table 3. Collection of Magnetic Data for the Compounds **1**, **2**, **4**, and **5**[a]

	unit	*Z*	*C* (calc) $cm^3 mol^{-1} K$	*C* CW fit $cm^3 mol^{-1} K$	θ (K)	T_{min} (K)	T_{max} (K)	T_{ac} (K)	T_N (K)	Ms ($N\beta$) theory	Ms ($N\beta$) obs	H_c kOe	meta-magnet
1	$MnCr_2$	8/3	8.125	8.3	−91.4	17	5.5	3.5	3.2	1	1.1	3.0	yes
2	$MnCr_2$	2	8.125	7.9	−66.8			2.3	2.3	1	1.2	4.0	yes
4	MnCr	2	6.25	6.5	−37.6	16	4.3	2.1	2.1	2	2.2	1.0	yes
5	MnCr	3	6.25	6.3	−41.5	26	7.7	5.1	4.7	2	2.1	4.9	yes

[a] *Z* is the average neighbor number of the metal ion through a cyanide bridge. H_c is the critical field for AF state to ferrimagnetic state.

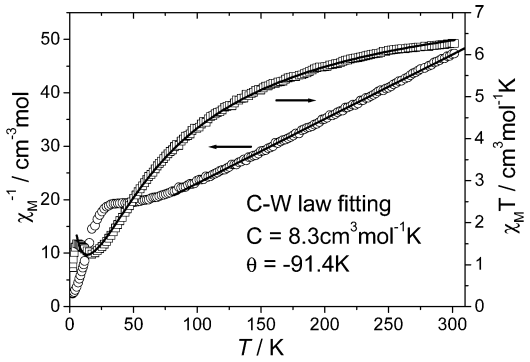

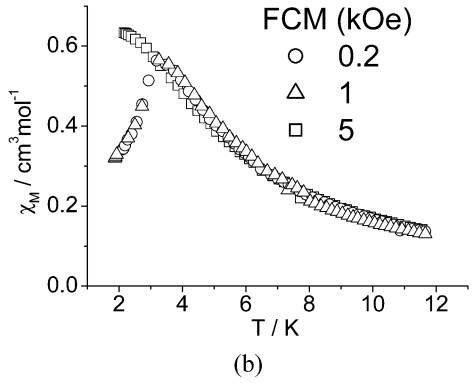

Figure 7. (a) $\chi_M T$ (square) and $1/\chi_M$ (circle) vs *T* in an applied field of 10 kOe for **1**. The solid lines correspond to the best fit to the Curie−Weiss law and the best fit with an alternating-chain model. (b) χ_M vs *T* plots at different fields.

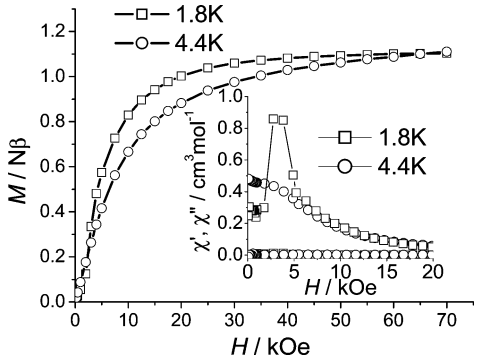

Figure 8. Field-dependent magnetizations for **1** at 1.8 and 4.4 K. Inset: Field-dependent *ac* susceptibilities at 1.8 and 4.4 K.

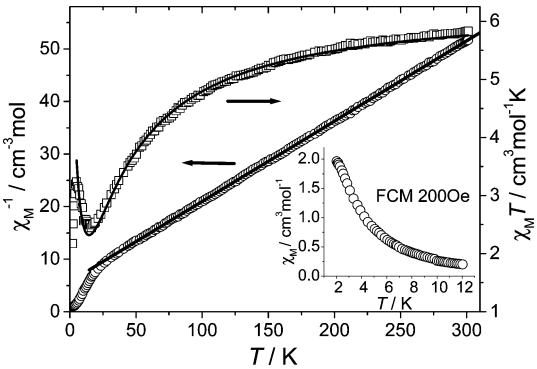

Figure 9. $\chi_M T$ (square) and $1/\chi_M$ (circle) vs *T* in an applied field of 10 kOe for **4**. The solid lines correspond to the best fit to the Curie−Weiss law and the best fit to the alternating-chain model. Inset: FCM at 200 Oe.

of compound **4** because of the terminal anion dca. Upon examination of the 2D compound bridged by cyanide and azide,[17] we found that the $\pi-\pi$ stacking from the middle phenyl cycles of phen plays an important role in stablizing the structure. Thus, when azide was introduced to the system of $Mn^{II} + [Cr(bpy)(CN)_4]^-$, the tendency was to form another structure without the $\pi-\pi$ stacking, and a novel 1D ladder-like compound **5** was self-assembled. To the best of our knowledge, the mer-mode of this class of tetracyanometalates has not been previously observed. When additional 2,2′-bpy was added (Mn^{II}/bpy/N_3 = 1:1:10), a snippet of **5** was obtained as $\{Mn(bpy)(N_3)\ [Cr(bpy)(CN)_4]\}_2$ (**6**), which is a square with alternating Mn and Cr units. As a result, three genuine examples (**3**, **4**, **6**) were rationally synthesized. As far as we know, compound **5** is the first cyano-bridged, neutral, real-spin 3,3-ladder complex.

Magnetic Studies. Magnetic Properties of 1, 4, and 5. Magnetic susceptibilities of the crystalline samples **1**, **4**, and **5** were measured in the range of 2−300 K. The results indicate that their magnetic behaviors are very similar, that is, they all show metamagnetic behavior. Therefore, only **5** will be described in some details here as an example. The main magnetic results have been listed in Table 3. The magnetic data of **1** and **4** are shown in Figures 7, 8, and S5 (Supporting Information) and Figures 9, 10, and S6 (Supporting Information), respectively. As shown in Figure 11a, the magnetic susceptibility for compound **5** above 50 K obeys the Curie−Weiss law [$\chi_M = C/(T - \Theta)$] and gives the Weiss constant $\Theta = -41.5$ K and the Curie constant $C = 6.27$ cm^3 mol^{-1} K. The *C* value is consistent with the expected value of 6.25 for a sum of isolated spin-only ions in a $Mn^{II}Cr^{III}$ unit ($g = 2$). The negative Θ indicates a dominant antiferromagnetic (AF) coupling between the Cr^{III} and Mn^{II} ions in this compound. As the temperature is lowered, the $\chi_M T$ value decreases gradually and reaches a minimum at ∼26 K, then increases abruptly, suggesting a ferrimagnetic character. $\chi_M T$

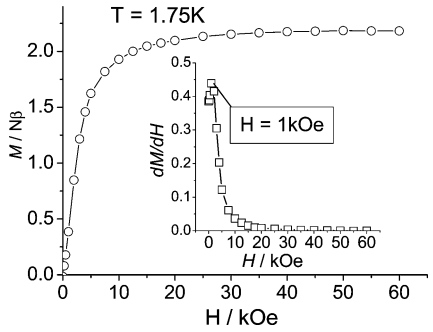

Figure 10. Field-dependent magnetizations for **4** at 1.75 K. Inset: d*M*/d*H* vs *H* plot.

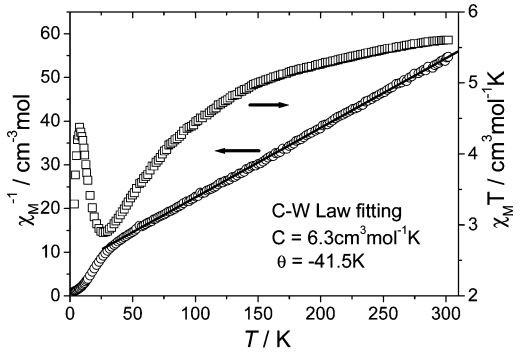

(a)

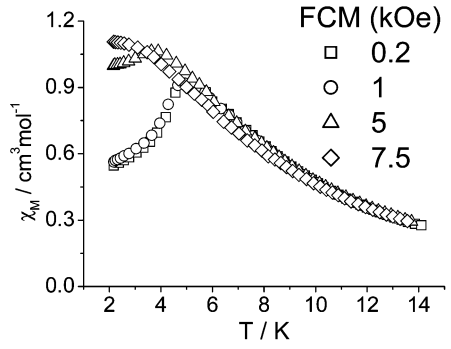

(b)

Figure 11. (a) $\chi_M T$ (square) and $1/\chi_M$ (circle) vs T in an applied field of 10 kOe for **5**. The solid line corresponds to the best fit to the Curie−Weiss law. (b) χ_M vs T plots at different fields.

reaches a maximum value at ∼6 K and then decreases sharply, which might be caused by magnetic saturation and/or AF interactions between the ferrimagnetic chains and/or zero-field splitting (ZFS). The field-cooled magnetization (FCM) at 200 Oe (Figure 11b) and the real part of *ac* susceptibility at different frequencies (277, 666, 1633, and 4111 Hz) in a zero *dc* field (Supporting Information Figure S7) display maxima at ∼5.0 K, in which the out-of-phase component (χ'') remains zero, thereby suggesting an AF ordering. The transition temperature (T_N) can be estimated as 4.7 K by the maximum of d($\chi_{ac}T$)/dT at 666 Hz. The maximum in $\chi_M T$ disappears when the applied field is larger than 7.5 kOe, suggesting a metamagnetic behavior (Figure 11b). The field-dependent magnetization at 1.8 K shows a pronounced sigmoid behavior: the magnetization first increases slowly as the field increases because of AF interchain interactions, then

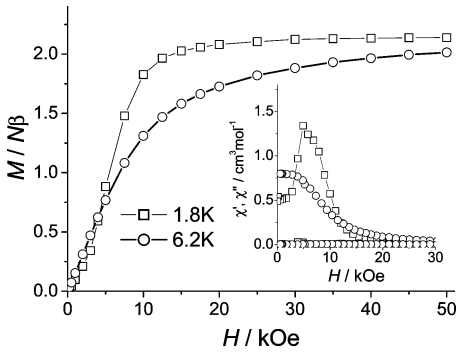

Figure 12. Field-dependent magnetizations for **5** at 1.8 and 6.2 K. Inset: Field-dependent *ac* susceptibilities at 1.8 and 6.2 K.

Scheme 3

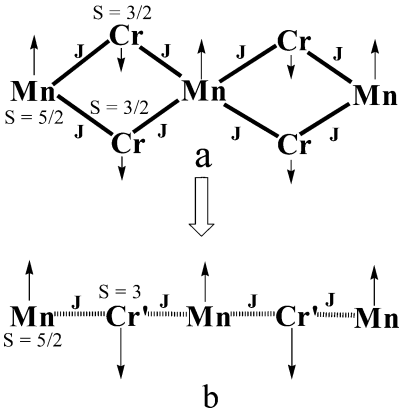

sharply transitions to a ferrimagnetic state (Figure 12). The magnetization value is 2.14$N\beta$ mol^{-1} at 50 kOe and 1.8 K, which is consistent with the expected ferrimagnetic state $S_T = 5/2 - 3/2 = 1$ for a MnCr unit. The H_c is ∼4.9 kOe at 1.8 K, which is estimated from the sharp peak of the field-dependent *ac* susceptibility (inset of Figure 12).

The magnetic behaviors of **1**, **4**, and **5** can be rationalized on the basis of their molecular structures. The noncompensation between the AF-coupled spins of Mn^{II} and Cr^{III} ions, which depends on whether the structure has a Cr/Mn = 2 chain for **1** or a Cr/Mn =1 chain for **4** and **5**, leads to ferrimagnetic behavior. The same approach used previously was applied to analyze **1** (Scheme 3).[17] The Hamiltonian for compound **1** is as follows (intrachain coupling J):

$$H = -J\sum_{i=1}^{N}(S_{\mathrm{Mn},i}\cdot S_{\mathrm{Cr},i+1}^{\mathrm{upper}} + S_{\mathrm{Mn},i}\cdot S_{\mathrm{Cr},i+1}^{\mathrm{lower}}) = -J[S_{\mathrm{Mn},i}\cdot(S_{\mathrm{Cr},i+1}^{\mathrm{upper}} + S_{\mathrm{Cr},i+1}^{\mathrm{lower}})] \quad (1)$$

If $S_{\mathrm{Cr},i+1}^{\mathrm{upper}} + S_{\mathrm{Cr},i+1}^{\mathrm{lower}} = S'_{\mathrm{Cr},i+1}$ is the effective spin of Cr ions on sites of $i + 1$, and $H = -J\sum_{i=1}^{N}(S_{\mathrm{Mn},i}\cdot S'_{\mathrm{Cr},i+1})$ is the spin quantum number $S_{\mathrm{Cr}}^{\mathrm{upper}} = S_{\mathrm{Cr}}^{\mathrm{lower}} = 3/2$, then the effective spin number S'_{Cr} could be 3, 2, 1, or 0. Because all observed Mn−Cr coupling through CN is always AF, and because there is no detected interaction between the neighboring Cr^{III} ions, all Cr^{III} ions have the same directional alignment, and therefore 3 is a reasonable value for the ground-state spin of S'_{Cr}. Thus, both **1** and **4** can be described by the alternating chain model [$H = -J\sum_{i=1}^{N}(S_{\mathrm{Mn},i}\cdot S'_{\mathrm{Cr},i+1})$ for **1** and

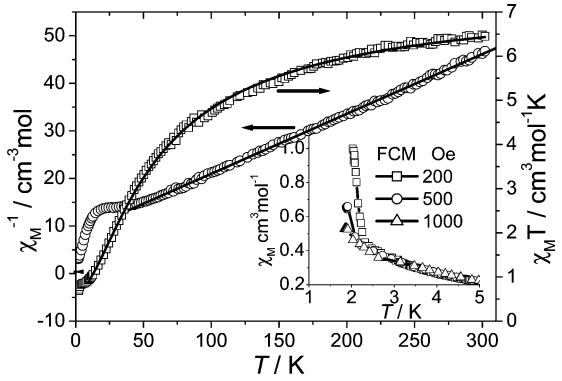

Figure 13. $\chi_M T$ (square) and $1/\chi_M$ (circle) vs T in an applied field of 10 kOe for **2**. The solid lines correspond to the best fit to the Curie−Weiss law and an approximate alternating-chain model. Inset: χ_M vs T plots at different fields.

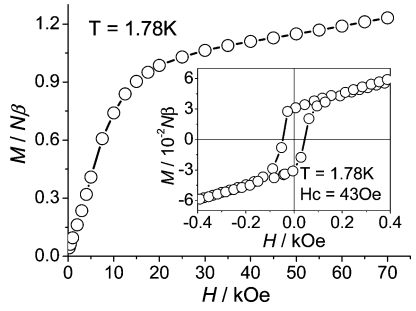

Figure 14. Field-dependent magnetizations for **2** at 1.8 K. Inset: Hysteresis loop at 1.8 K for **2**.

$H = -J\sum_{i=1}^{N}(S_{Mn,i}\cdot S_{Cr,i+1})$ for **4**]. The best fitting of the magnetic data above 5 K (above T_N) together with a molecular field approach that includes the interchain magnetic interaction (zJ') gives the following results: $J = -6.4$ cm^{-1}, $J' = -2.7/z$ cm^{-1} $= -0.45$ cm^{-1} ($z = 6$), $g_{Cr} = 2.02$, and $g_{Mn} = 2.00$ with $R = 9.6 \times 10^{-5}$ for **1**; $J = -5.4$ cm^{-1}, $J' = -0.79/z$ cm^{-1} $= -0.13$ cm^{-1} ($z = 6$), $g_{Cr} = 2.04$, and $g_{Mn} = 2$ with $R = 2.1 \times 10^{-4}$ for **4** $\{R = \sum[(\chi_M T)_{obs} - (\chi_M T)_{calc}]^2/\sum(\chi_M T)_{obs}^2\}$[20] ($J'$ = interchain coupling′). Using this approximate approach, we found that the fitting result for **1** (-6.4 cm^{-1}) is very consistent with the Monte Carlo simulation (-7.5 cm^{-1}) for the same compound performed by Julve and co-workers.[16b] The AF interactions between the nearest chains (negative zJ') result in an AF ground state, which turns into a ferrimagnetic state at higher fields; thus the compounds exhibit metamagnetic behaviors: the bigger the zJ', the higher the critical field.

Magnetic Properties of 2. The temperature dependence of $\chi_M T$ in the range of 2−300 K for compound **2** ($MnCr_2$ unit) is presented in Figure 13. The magnetic susceptibility above 70 K obeys the Curie−Weiss law and gives the Weiss constant $\Theta = -66.8$ K and the Curie constant $C = 7.94$ cm^3 mol^{-1} K. The C value is consistent with the expected value of 8.125 for a sum of isolated spin-only ions in Mn^{II}-Cr^{III}_2 ($g = 2$). As the temperature is lowered, the $\chi_M T$ value decreases gradually and reaches a plateau at ∼10 K, then decreases abruptly at ∼3 K, which may be due to interchain AF coupling and/or ZFS and/or magnetic saturation effects. Long-range magnetic ordering is clearly evidenced by low-field magnetization and *ac* susceptibility measurements. As shown in the inset of Figure 13, remarkable field dependence is observed. At 200 Oe, a spontaneous magnetization occurs as a result of spin canting, which gradually disappears at 500 and 1000 Oe. The real part of *ac* susceptibility at different frequencies (277, 666, 1633, and 4111 Hz) in the absence of a *dc* field (Supporting Information Figure S8) displays spiculate peaks with a slight frequency dependence at ∼2.3 K, whereas the out-of-phase component (χ'') almost vanishes. T_N can be estimated to be 2.3 K and characterized by the maximum of $\chi'_{ac}T$ vs T at 666 Hz. The isothermal magnetization $M(H)$ as a function of the field up to 70 kOe was measured at 1.8 K, as shown in Figure 14. At low fields, the magnetization rises rapidly below 100 Oe (inset of Figure 14) then increases almost linearly to 4 kOe, which corresponds to an AF state, and then increases rapidly to a ferrimagnetic state. This is further evidenced by a clear discontinuity in the dM/dH curve at 4 kOe (Supporting Information Figure S9). The magnetization value is $1.2N\beta$ at 70 kOe and 1.8 K, which is consistent with the expected ferrimagnetic state $S_T = (2 \times 3/2) - 5/2 = 1/2$ for a $MnCr_2$ unit. As shown in the inset of Figure 14, an unusual hysteresis curve was observed with a coercive field of 43 Oe and a remanent magnetization of $0.03N\beta$ mol^{-1}. From this observation, we can estimate that the spin canting angle, γ, is 0.16°. To affirm its unusual magnetic properties, detailed zero-field-cooled magnetization (ZFCM) and FCM measurements were performed on a SQUID magnetometer, as shown in Supporting Information Figures S10 and S11. The ZFCM and FCM at 20 Oe are divergent below 2.04 K, whereas the FCMs, which depend dramatically on the field below 2.04 K, were saturated at 100 and 500 Oe and at 1 and 2 kOe. These behaviors strongly suggest the occurrence of spin canting. A maximum appears at 2.1 K when the field is higher than 2 kOe (3 kOe, 4 kOe) and disappears at a higher field (6 kOe), which is a typical property of a metamagnet. The spin canting leads to a weak ferromagnetic ground state, and at fields higher than 4 kOe it turns into a ferrimagnetic state. Therefore, the compound exhibits canting and metamagnetic behaviors.[21] Although there is no local single-ion anisotropy for high-spin Mn^{II} and low-spin Cr^{III} in this system, the spin canting may arise from the antisymmetric exchange of Cr−Mn because of the lack of a center of symmetry between Cr and Mn. This Dzyaloshinski−Moriya interaction is a reasonable explanation for the canting in **2**.[22]

An approximate approach has been widely used for 1D, 2D, and quasi-2D complexes to roughly estimate the J value.[9a,23] In terms of the crystal data, the Cr−CN−Mn linkages are quite different in **2**. Therefore, the 1D chain can be treated as alternating uniform Cr_1Mn dimers (Cr_1 from the branch) and Cr_2 posessing different intradimeric and

(20) Kahn, O. *Molecular Magnetism*; VCH: Weinheim, Germany 1993.

(21) Nocera, D. G.; Bartlett, B. M.; Grohol, D.; Papoutsakis, D.; Shores, M. P. *Chem.—Eur. J.* **2004**, *10*, 3851 and references therein.

(22) (a) Carlin, R. L.; Van-Duyneveldt, A. J. *Magnetic Properties of Transition Metal Compounds*; Springer-Verlag: New York, 1977. (b) Armentano, D.; De Munno, G.; Mastropietro, T. F.; Julve, M.; Lloret, F. *Chem. Commun.* **2004**, 1160.

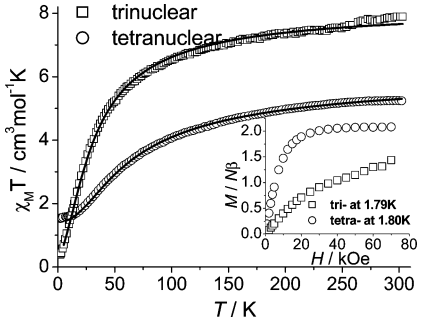

Figure 15. $\chi_M T$ vs T in an applied field of 10 kOe for **3** (square) and **6** (circle). The solid lines correspond to the best fit to the linear trinuclear of Cr−Mn−Cr and square $[CrMn]_2$ models for **3** and **6**, respectively. Inset: Field-dependent magnetizations at ∼1.8 K.

intrachain exchange constants (J_d vs J_c): $H = -J_d S_{Mn} \cdot S_{Cr1}$ (dimer); $H = -J_c S_d \cdot S_{Cr2}$. Here

$$\chi_d = [Ng^2\beta^2/3kT]\,[180\exp(3.75J_d/kT) + 84\exp(-0.25J_d/kT) + 30\exp(-3.25J_d/kT) + 6\exp(-5.25J_d/kT)]/[9\exp(3.75J_d/kT) + 7\exp(-0.25J_d/kT) + 5\exp(-3.25J_d/kT) + 3\exp(-5.25J_d/kT)], \quad (2)$$

$$\chi_d = \frac{Ng^2\beta^2}{3kT} S_d(S_d+1) \text{ (for a classical spin system)}, \quad (3)$$

$$\chi_{chain} = \frac{N\beta^2}{3kT}\left[g^2\frac{1+u}{1-u} + \delta^2\frac{1+u}{1-u}\right], \quad (4)$$

$g_A^e = g_{Cr}[S_{Cr}(S_{Cr}+1)]$, $g_B^e = g_d[S_d(S_d+1)]$, $g = (g_A^e + g_B^e)/2$, and $\delta = (g_A^e - g_B^e)/2$; $u = \coth(J^e/kT) - (kT/J^e)$, in which $J^e = J_c[S_{Cr2}(S_{Cr2}+1)S_d(S_d+1)]^{1/2}$. On the basis of this approximate model, the best fitting (10−300 K) gives: $J_d = -9.4$ cm^{-1}, $J_c = -4.8$ cm^{-1}, $g_{Cr} = g_d = g_{Mn} = 1.92$ and $R = 1.4 \times 10^{-4}$ $\{R = \sum[(\chi_M T)_{obs} - (\chi_M T)_{calc}]^2/\sum(\chi_M T)_{obs}^2\}$.

Magnetic Properties of 3 and 6. The temperature dependence of $\chi_M T$ in the range of 2−300 K for crystalline samples of **3** ($MnCr_2$ unit) and **6** (MnCr unit) is presented in Figure 15. As the temperature is lowered, the $\chi_M T$ value decreases gradually, suggesting the presence of an AF coupling between the adjacent Mn and Cr ions. The magnetic susceptibility above 50 K obeys the Curie−Weiss law with Curie (cm^3 mol^{-1} K) and Weiss (K) constants $C = 8.44$ and $\Theta = -29.4$ for **3** and $C = 6.22$ and $\Theta = -53.1$ for **6** (Supporting Information Figure S12). The C values are consistent with the calculated value of 8.125 expected for a sum of isolated spin-only ions in $Mn^{II}Cr^{III}_2$ ($g = 2$) and the calculated value of 6.25 expected for a sum of isolated spin-only ions in $Mn^{II}Cr^{III}$. The magnetization value is $1.44N\beta$ mol^{-1} at 70 kOe and 1.8 K for **3**, which is slightly higher than the expected value for the AF state of $MnCr_2$ $S_T = (3/2 \times 2 - 5/2) = 1/2$ (inset of Figure 15). The M(H) as a function of the field is also measured at 1.8 K for **6**. The value of $2.08N\beta$ at 70 kOe is consistent with the expected value for the AF state of MnCr $S_T = (5/2 - 3/2) = 1$. According to the crystal data of **3**, we can assume that there is only one exchange mode ($Mn^{II}-CN-Cr^{III}$, though $\angle Mn_1-N_4-C_4 = 170.6$, but $\angle Mn_1-N_{11}-C_{35} = 164.9$), and that the magnetic interaction between Cr ions can be neglected for simplicity because of the long distance between Cr1 and Cr2. Thus, the appropriate Hamiltonian would be $H = -J(S_{Cr1}\cdot S_{Mn1} + S_{Cr2}\cdot S_{Mn1})$, in which J is the coupling constant through the cyano bridges. By means of Kambe's method,[24] the data are fitted, and the corresponding results are obtained: $J = -5.2$ cm^{-1}, $g = g_{Cr} = g_{Mn} = 2.01$, and $R = 1.8 \times 10^{-4}$.

Until recently, there were a few compounds bridged by cyanide groups with a square struture,[15,25] but only three of them were pure squares.[15a,15e,25] The three compounds have been analyzed by the four spin model. In Fe_2Cu_2, the magnetic interactions (J_2) between the diagonal Fe···Fe and Cu···Cu bonds were considered, which resulted in the value -3.1 cm^{-1}, whereas the magnetic interaction (J_1) between Fe···Cu through the cyano-bridge was 6 cm^{-1}. In this case, the ferromagnetically coupled Fe and Cu should be affected by the AF coupling from the diagonal interaction, and spin frustration may exist. However, no evidence was found to prove this presumption. In Gd_2Mn_2, the diagonal interactions were neglected, which resulted in a value of $J_1 = -0.36$ cm^{-1}. According to the crystal structure of **6**, we can assume that there might be equivalent coupling constants because there is little difference between $Cr-C_1-N_1-Mn$ and $Cr-C_3-N_3-Mn$ and that the diagonal magnetic interactions between Cr ions or Mn ions may be neglected. Thus, the appropriate Hamiltonian can be of the form: $H = -J(S_{Cr1}\cdot S_{Mn1} + S_{Mn1}\cdot S_{Cr2} + S_{Cr2}\cdot S_{Mn2} + S_{Mn2}\cdot S_{Cr1})$, in which J is the coupling through the cyano bridges. Following the Kambe's method,[24] one can obtain the corresponding fitting results ($g_{Cr} = g_{Mn} = 2.0$): $J = -8.0$ cm^{-1}with $R = 7 \times 10^{-5}$.

In cyanide magnets, some rough rules have been documented, which include (1) the cyano group can transmit the magnetic interactions between transition metal ions ferromagnetically or antiferromagnetically, depending on the symmetry of the magnetic orbitals;[20] (2) the direct exchange interactions between transition metal ions are almost zero as their distances are larger than 5 Å; (3) the magnetic phase transition temperature T_c follows the following equation:[26]

$$T_c = \frac{2}{k} y\sqrt{y}|J|\sqrt{S_M(S_M+1)S_{M'}(S_{M'}+1)};$$

and (4) $J_{MM'}$ can be estimated by[27]

$$J_{MM'} = \frac{1}{mn}[\sum_{i=1}^{m}\sum_{j=1}^{n} J_{ij}].$$

(23) (a) Caneschi, A.; Gatteschi, D.; Melandri, M. C.; Rey, P.; Sessoli, R. *Inorg. Chem.* **1990**, *29*, 4228. (b) Chiari, B.; Cinti, A.; Piovesana, O.; Zanazzi, P. F. *Inorg. Chem.* **1995**, *34*, 2652. (c) Wrzeszcz, G.; Dobrzañska, L.; Wojtczak, A.; Grodzicki, A. *J. Chem. Soc., Dalton Trans.* **2002**, 2862.

(24) Kambe, K. *J. Phys. Soc. Jpn.* **1950**, *5*, 48.

(25) Kou, H. Z.; Gao, S.; Li, C. H.; Liao, D. Z.; Zhou, B. C.; Wang, R. J.; Li, Y. D. *Inorg. Chem.* **2002**, *41*, 4756.

(26) Ferlay, S.; Mallah, T.; Ouahès, R.; Veillet, P.; Verdaguer, M. *Inorg. Chem.* **1999**, *38*, 229.

(27) Ohkoshi, S.; Hashimoto, K. *Chem. Phys. Lett.* **1999**, *314*, 210.

Table 4. Structural and Magnetic Parameters for Related Cr−Mn Cyanide Compounds

	Mn−N−C−Cr (deg)			
compound	Mn−N−C	Cr−C−N	J/cm^{-1}	ref
1	139.6	172.8	−6.4	this work
	140.9	169.2		
2	154.9	169.2	−9.4	
	173.5	174.8	−4.8	this work
	170.0	176.5		
3	164.9	176.7	−5.2	this work
	170.7	176.3		
4	172.7	173.7	−5.4	this work
	173.0	175.9		
6	161.3	174.7	−8.0	this work
	161.9	178.5		
Cr_2Mn-phen	174.9	160.5	−4.7	17
	175.7	160.5		
[$CrMn_6$]	161.7		−7.2	11
	153.6		−10.5	
$MnCr_6$−**1**	152.7	177.2	−6	14d
$MnCr_6$−**2**	153.4	176.5	−6.2	14d
Mn_3Cr_6−**3**	173.4	176.1	−6.0	14d
	167.2			
$MnCr_3$−**4**	164.7	176.1	−6.6	14d
3D-NaCrMn	180	180	−3.6	28
$MnCr_2$	168.9	170.7	−6.2	16b

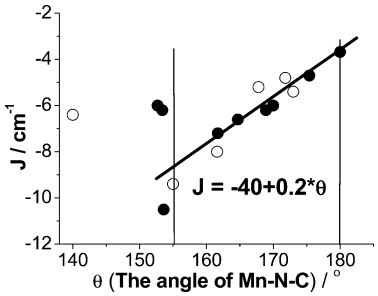

Figure 16. The coupling constant (*J*) plotted against the angle of Mn−N−C (θ°). The open symbols stand for the data in this work and the solid ones for the reported data in the literature. The red line corresponds to the linear fitting.

Obviously, the detailed factors such as the deviation of Mn−N−C−Cr from the linearity have been ignored in the studies mentioned above for simplicity. Julve and co-workers recently reported four Cr−Mn compounds based on [Cr(bpy)-$(CN)_4$]$^-$ and used Monte Carlo simulation and DFT type calculations to analyze some of the magnetic behaviors. They concluded that the larger AF coupling corresponds to the higher bending of the Cr−C−N−Mn unit.[16b] The relationship between the angle of M−N−C (θ/°) and the Mn−Cr coupling constant (*J*) is also observed in this work. The t_{2g}−t_{2g} pathways are ensured to transfer the AF coupling between the $t_{2g}^3e_g^2$ high-spin Mn^{II} and the $t_{2g}^3e_g^0$ Cr^{III} involved in all the title compounds. The magnetic analyses demonstrate that the intermetallic magnetic exchange constant *J* is between −4.7 and −9.4 cm^{-1}, which, together with the previous results,[14d,16b,28] is documented in Table 4. Figure 16 shows the plot of *J* versus θ using the data in this table. It is found that the AF coupling increases almost linearly as the angle of Mn−N−C decreases from 180° to 155°, obeying an approximate relationship: J(cm^{-1}) = −40 + 0.2θ. When the angle deviates from a collinear arrangement, the overlap of two coupling orbitals probably increases, and consequently an increase in J_{AF} will follow. However, a large deviation (θ < 155°) may reduce this overlap, and the simple linear relation between *J* and θ is no longer preserved. On the basis of the data collected in Table 4 and Figure 16, the Mn−N−C angle at 155° may give the best overlap between t_{2g}-(high-spin Mn^{II}) and t_{2g}(low-spin Cr^{III}). On the other hand, our experimental data appear to follow a general rule that the average number (*Z*) of nearest neighbors for metal ions determines the critical temperature whose value is in the order: **5** (Z = 3) > **1** (Z = 8/3) > **2** (Z = 2) ≈ **4** (Z = 2).

Conclusion

In this paper, we have succeeded in developing a rational synthesis of some low-dimensional bimetallic cyanides with interesting magnetic properties. Three routes with gradual modification have been achieved by introducing a suitable secondary and/or tertiary coligand: (1) 4,2-ribbon chain - - - branched zigzag chain - - - trinuclear; (2) 4,2-ribbon chain - - - branched zigzag chain - - - pure zigzag 2,2-CC chain; (3) 4,2-ribbon chain - - - 3,3-ladder chain - - - square tetranuclear. Magnetic studies have shown that the coupling between Mn^{II} and Cr^{III} ions in all the title compounds are AF, and the *J* values of the different compounds were estimated to be in a range of −4.7 to −9.4 cm^{-1}. It has been found that the AF coupling (*J*) follows an approximate relationship in the range of θ = 155−180°: J(cm^{-1}) = −40 + 0.2θ, in which θ (°) is the angle of Mn−N−C deviated from the Mn−N−C−Cr bridge. The 1D compounds (**1**, **2**, **4**, and **5**) exhibit metamagnetic behaviors below the temperature range of 2.1−4.7 K, and their transition temperatures depend on the average number of neighbors for metal ions. Additionally, the noncentrosymmetric compound **2** shows weak ferromagnetism.

Finally, it is noteworthy that (1) the chelating ligand L of [M(L)$(CN)_4$]$^-$ can affect the target products, therefore [M(L)$(CN)_4$]$^-$ should be studied further to expand this remarkable field; (2) tetra-geometry may behave as a potential tool to build the 4,2-tubular molecules; (3) the alternating building block is a good ligament to study complexes with mixed effective magnetic bridges; (4) it will be interesting to explore the assembled compounds with other 3d metal ions, such as Co^{II}, Cu^{II}, Ni^{II}, etc.; and (5) more examples are needed to examine and interpret the relationship between *J* and θ. In a word, the addition of a second or even a third coligand sheds some light on the big challenge of the rational design of low-dimensional magnetic molecular materials.

Experimental Section

General Remarks. All starting materials were commercially available, reagent grade, and used as purchased without further purification. Elemental analyses of carbon, hydrogen, and nitrogen were carried out with an Elementary Vario EL. The IR spectra were recorded against pure samples on a Magna-IR 750 spectrophotometer in the 4000−500 cm^{-1} region. The measurements of variable-temperature magnetic susceptibility, zero-field *ac* magnetic susceptibility, and field dependence of magnetization were performed

(28) Dong, W.; Zhu, L. N.; Song, H. B.; Liao, D. Z.; Jiang, Z. H.; Yan, S. P.; Cheng, P.; Gao, S. *Inorg. Chem.* **2004**, *43*, 2465.

on an Oxford Maglab^{2000} System and a SQUID magnetometer. The experimental susceptibilities were corrected for diamagnetism (Pascal's tables).

Synthesis. The precursor [Cr(bpy)$_2$(CN)$_2$][Cr(bpy)(CN)$_4$] (abbreviated as Cr^{2,4}) was prepared by the literature method.[29] An improved strategy gave a new product of Na(bpy)(H$_2$O)[Cr(bpy)(CN)$_4$] (abbreviated as Na−Cr^4).[30]

Caution!: Although it was not encountered in our experiments, azide salts are potentially explosive. Only a small amount of the materials should be prepared, and it should be handled with care.

(1) A bright yellow solution of Cr^{2,4} (0.1 mmol) in methanol/H$_2$O (10:5 mL) was mixed with an aqueous solution (5 mL) of MnCl$_2$ (0.1 mmol). The resulting solution was left to stand at room temperature. Yellow blocked single crystals of **1** were obtained after several days. Yield: 30 mg, 84%. Anal. Calc. for MnCr$_2$C$_{28}$H$_{20}$N$_{12}$O$_2$ (%): C, 47.00; H, 2.82; N, 23.49. Found: C, 46.93; H, 3.18; N, 24.01. IR stretching cyanide (cm^{-1}): 2144 (sharp peak, m).

(2) A bright yellow solution of Na−Cr^4 (0.1 mmol) in methanol/H$_2$O (5:5 mL) was poured into a test tube. Then 10 mL of methanol and 5 mL of a methanol solution of MnCl$_2$ (0.1 mmol) were layered above it. Yellow plate single crystals of **2** were obtained after a month. Yield: 16 mg, 36%. Anal. Calc. for MnCr$_2$C$_{38}$H$_{28}$N$_{14}$O$_2$ (%): H, 3.24; C, 52.36; N, 22.50. Found: H, 3.45; C, 52.18; N, 22.32. IR stretching azide and cyanide (cm^{-1}): 2151, 2166 ($\nu_{C\equiv N}$, w). The identity of the product used in magnetic measurements was confirmed by powder X-ray diffraction analysis (Supporting Information Figure S13).

(3) Method A: MnCl$_2$ (0.1 mmol) and bpy (0.2 mmol) were dissolved in methanol/H$_2$O (10:5 mL), stirred for 30 min, and then mixed slowly with a bright yellow solution of Cr^{2,4} (0.1 mmol) in 10 mL of methanol. The resulting solution was left to stand at room temperature. Yellow column single crystals of **3** were obtained after several days. Yield: 40 mg, 74%. Anal. Calc. for MnCr$_2$C$_{48}$H$_{44}$N$_{16}$O$_5$ (%): C, 53.19; H, 4.09; N, 20.68. Found: C, 53.51; H, 3.75; N, 21.11. IR stretching azide and cyanide (cm^{-1}): 2157, 2167 ($\nu_{C\equiv N}$, w). Method B: **2** (20 mg, 0.023 mmol) was dissolved in methanol/H$_2$O (10:5 mL) and was then mixed slowly with a bright solution of 2,2′-bpy (0.05 mmol) in 2 mL of methanol. The resulting solution was left to stand at room temprature. Yellow column single crystals of **3** were obtained after several days. Yield, 15 mg, 60%. Anal. Calc. Found (%): C, 53.43; H, 3.87; N, 20.92. The crystals were confirmed by X-ray analysis.

(4) Fifteen milliliters of a methanol solution of MnCl$_2$ (0.1 mmol) and dca (1 mmol) was stirred for several hours and was then mixed slowly with an bright yellow solution of Na−Cr^4 (0.1 mmol) in methanol/H$_2$O (10:5 mL). The resulting solution was left to stand at the room temperature. Yellow plate single crystals of **4** were obtained after several days. Yield: 25 mg, 40%. Anal. Calc. for MnCrC$_{26}$H$_{20}$N$_{11}$O$_2$ (%): C, 49.93; H, 3.22; N, 24.63. Found: C, 50.04; H, 3.45; N, 24.98. IR stretching dicyanamide and cyanide (cm^{-1}): 2172 (vs), 2242, 2299(m) corresponding to ν_{dca}; ν_{CN} was concealed.

(5) Fifteen milliliters of a methanol solution of MnCl$_2$ (0.1 mmol) and NaN$_3$ (1 mmol) was stirred for several hours (which is necessary) and was then mixed slowly with a bright yellow solution of Cr^{2,4} (0.1 mmol) in methanol/H$_2$O (10:5 mL). The resulting solution was left to stand at room temperature. Yellow block single crystals of **5** were obtained after several days. Yield: 30 mg, 61%. Anal. Calc. for MnCrC$_{15}$H$_{18}$N$_9$O$_4$ (%): C, 36.37; H, 3.66; N, 25.45. Found: C, 36.54; H, 3.47; N, 25.58. IR stretching azide and cyanide (cm^{-1}): 2079 (ν_{azide}, vs), 2158 ($\nu_{C\equiv N}$, w, no splitting peaks because of the strong ν_{azide}).

(6) We prepared complex 6 using a procedure similar to that used for complex **4**, replacing dca with NaN$_3$. Yellow block single crystals of **6** were obtained after several days. Yield: 35 mg, 56%. Anal. Calc. for MnCrC$_{24}$H$_{22}$N$_{11}$O$_3$ (%): C, 46.54; H, 3.58; N, 24.87. Found: C, 46.48; H, 3.72; N, 24.90. IR stretching azide and cyanide (cm^{-1}): 2067, 2053 (ν_{azide}, vs), 2154 ($\nu_{C\equiv N}$, w)

X-ray Crystallographic Study: Crystallographic Data Collection and Structure Determination. The diffraction data collections of **1**−**5** were made at 293 K on a Nonius κ-CCD diffractometer and that of **6** was collected on a CCD area detector. The structures were solved by the direct method (SHELXS-97) and refined by full-matrix least squares (SHELXL-97) on F^2. Anisotropic thermal parameters were used for the non-hydrogen atoms. Hydrogen atoms were added geometrically, and a riding model was used to refine them. Weighted R factors (wR) and all of the goodness-of-fit (S) values were based on F^2; conventional R factors (R) were based on F, with F set to zero for negative F^2. The weighting scheme is $w = 1/[s^2F_0^2 + (0.0433P)^2 + 0.0000P]$, in which $P = (F_0^2 + 2F_c^2)/3$.

CCDC-246561 to 246566 contains the supplementary crystallographic data for this paper. These data can be obtained free of charge at www.ccdc.cam.ac.uk/conts/retrieving.html [or from the Cambridge Crystallographic Data Centre, 12, Union Road, Cambridge CB2 1EZ, UK; fax: (internat.) +44−1223/336−033; E-mail: deposit@ccdc.cam.ac.uk].

Acknowledgment. We acknowledge support from the National Science Fund for Distinguished Young Scholars (20125104), NSFC Nos. 20490210, 20221101, and 90201014 and the Research Fund for the Doctoral Program of Higher Education (20010001020).

Supporting Information Available: CIF files of **1**−**6**, plots of crystal packing for **1**, **2**, **4**, and **5** and more figures of magnetic data for **1**−**6**. This material is available free of charge via the Internet at http://pubs.acs.org.

IC0484194

(29) Ryu, C. K.; Endicott, J. F. *Inorg. Chem.* **1988**, *27*, 2203 and references therein.
(30) Zhang, Y. Z.; Gao, S.; Pan, F.; Wang, Z. M. Paper in preparation.